Extended Abstract, 20th Conf. Weather Analysis and Forecasting/
16th Conf. Numerical Weather Prediction
American Meteorological Society, Seattle, Washington, 2004

J8.2 INITIAL CONDITION SENSITIVITY ANALYSIS OF A MESOSCALE FORECAST USING VERY LARGE ENSEMBLES

William J. Martin[1,*] and Ming Xue[1,2]
[1]Center for Analysis and Prediction of Storms and [2]School of Meteorology
University of Oklahoma
Norman, Oklahoma 73019

1. INTRODUCTION

This work explores the sensitivity of mesoscale forecast fields to perturbations in the initial conditions. The mesoscale forecast is for the case of May 24, 2002 during the IHOP field experiment, a case which saw thunderstorms initiate in the afternoon along a dryline in the southwest Texas panhandle.

A mesoscale forecast model typically contains millions of degrees of freedom corresponding to the physical variables at each grid location. As a perturbation of any one of these variables can potentially have significant non-linear consequences, a complete exploration of this problem would require a model run for each perturbation of each degree of freedom. To examine nonlinearities, different sized perturbations also need to be explored for each of the millions of degrees of freedom in the model. Executing the many millions of model runs to test each possible perturbation of the model is not tenable with current computing technologies.

However, by making certain linearization assumptions, forecast sensitivities to initial model fields can be obtained by using a backward integration of an adjoint model (Errico, 1997). However, adjoint models have certain shortcomings including the complexity of implementing adjoint codes, large computer memory requirements, and the need to linearize the model around a nonlinear base state. The linearization assumptions can be particularly questionable when microphysics and other complicated physical processes are involved (Errico, 2003). Also, because perturbations often grow in time, the linearization assumptions inherent in an adjoint calculation become invalid if long time integration is involved. For these reasons, explorations of forecast sensitivities have often taken the approach of using a number of direct forward model integrations (e.g., Crook, 1996; Mullen and Baumhefner, 1994). These forward sensitivity analyses have been limited to a small number (10 to 100) of model runs, using essentially analytic perturbations of entire initial fields (rather than perturbing the initial fields at individual locations).

The new availability of large parallel computer systems with thousands of powerful processors makes it possible to run very large ensembles of a high-resolution mesoscale model. By restricting ourselves to perturbations of two dimensions in the initial field, a fairly complete sensitivity analysis of a forecast can be made from a couple thousand model runs, all of which can be done in parallel; and this is the approach taken in this paper. The forward mesoscale model is run over 2000 times with each run having a perturbation in the boundary layer moisture in a different horizontal location. All these model runs are executed in parallel simultaneously on a parallel supercomputer system. By this means, sensitivity analyses with greater detail than heretofore possible are obtained without the application and assumptions of an adjoint.

2. CASE AND METHODOLOGY

The initial condition analysis of the case to be analyzed is at 18Z on May 24, 2002 over a region of the southern Plains centered on Oklahoma. The initial field of surface water vapor over the entire domain is shown in Fig. 1 and the initial field of 10 m wind vectors is shown in Fig. 2. This analysis was obtained using the ADAS analysis package (Xue et al 2002; Xue et al. 2003) utilizing the standard National Weather Service rawinsondes, surface observations, with the NCEP ETA 18Z analysis as a background field. Additionally, special observations taken during the IHOP field program were used. They include aircraft dropsondes, and Kansas, Texas, and Oklahoma mesonet surface data. Many of these special observations were taken near the southwest corner of Oklahoma, north of where initiation actually occurred.

* *Corresponding author address:* William J. Martin, Center for Analysis and prediction of Storms, 100 East Boyd, SEC Room 1110, Norman, OK, 73019; wjmartin@ou.edu

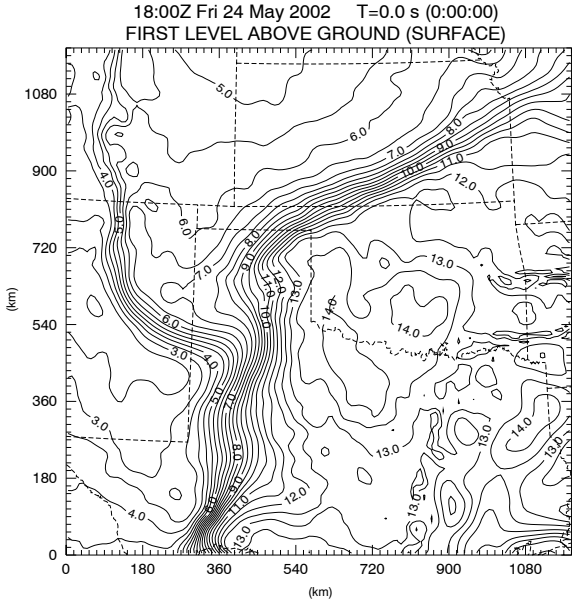

Fig. 1. Initial surface water vapor field in g kg^{-1} for May 24, 2002 at 18Z. Level is at 10 m above the ground.

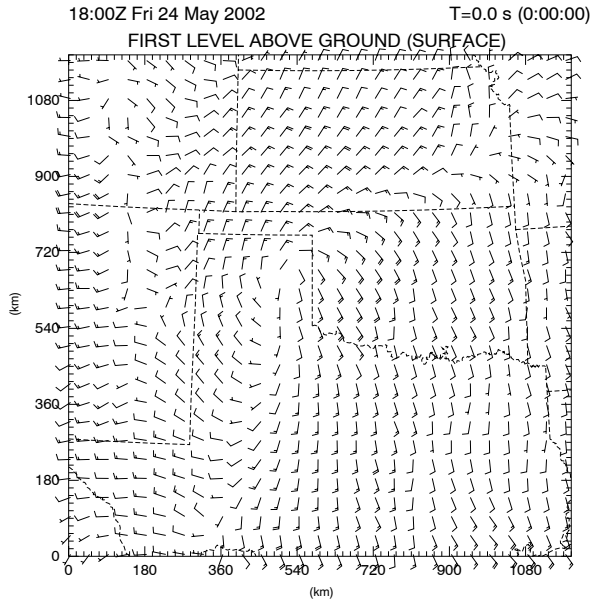

Fig. 2. Initial field of wind barbs for May 24, 2002 at 18Z, 10 m above the surface. One full wind barb is 5 m/s. A half wind barb is 2.5 m/s.

The analysis shows a generally north-south oriented dryline in the eastern Texas panhandle and an east-northeast to west-southwest oriented cold front across southern Kansas. This initial condition is integrated forward for 6 hours using the ARPS model (Xue et al. 2000) and lateral boundary forcing from the 18Z ETA forecast fields.

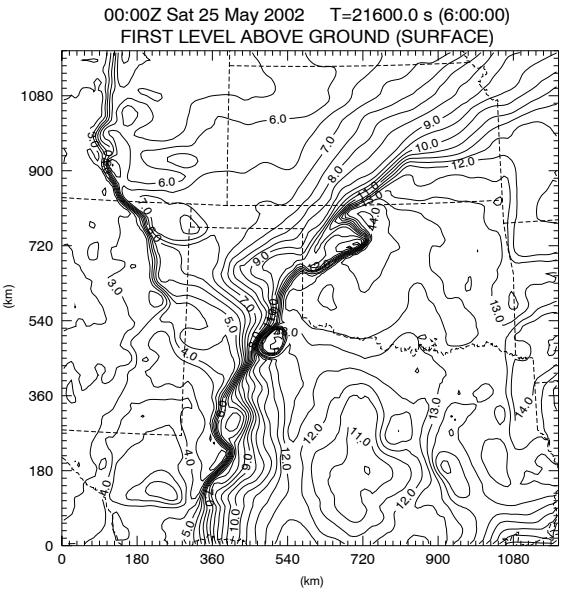

Fig. 3. 6 hour forecast water vapor field in g kg^{-1}, 10 m above the surface.

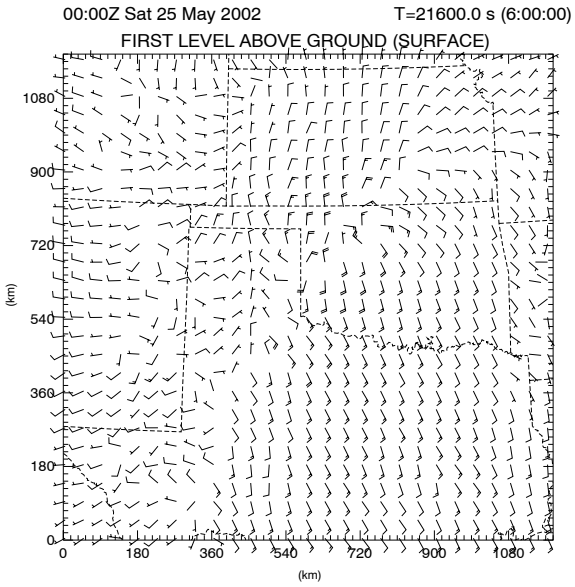

Fig. 4. 6 hour forecast field of 10 m wind barbs. Full wind barb corresponds to 5 m/s.

The numerical domain consists of 135 by 135 horizontal grid cells with 9 km grid spacing. There are 53 vertical grid levels on a stretched vertical grid with a minimum vertical spacing of 20 m at the surface. Despite the 9 km horizontal resolution, the model is integrated using an explicit representation of convection rather than a convective parameterization. Full ice, surface, and radiation microphysical packages are employed.

Six hour forecast fields of surface water vapor, 10 m wind barbs, and total accumulated precipitation are shown in Figs. 3, 4, and 5 respectively. After 6 hours of integration, the water vapor field shows a considerable amount of strengthening of the moisture gradient, and also shows the effects of convection along the cold front in northwest Oklahoma and near the dryline-cold front triple point in the southeast Texas panhandle. The actual weather on this day had convective initiation along the dryline very close to the location and time of this model forecast. However, the actual convection along the dryline developed into a much more intense storm system spreading much further south into west central Texas than was seen in this numerical model. Also, the precipitation along the cold front was negligible in the observations until much later than that seen here.

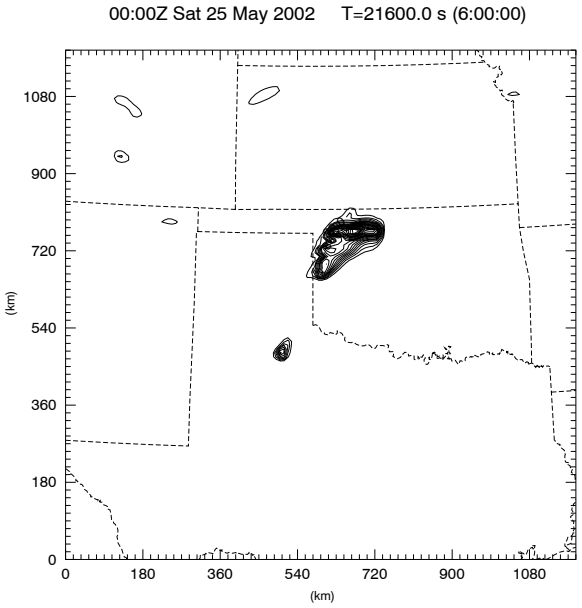

Fig. 5. 6 hour forecast of accumulated precipitation. Contour increments are 10 mm with a local maximum of 205 mm.

To investigate the sensitivity of this forecast to the initial water vapor field, the initial boundary layer moisture is perturbed at different locations and the model run from the perturbed initial condition for 6 hours. This is done for each of a large number of perturbations. To reduce the number of possible perturbation locations to consider, perturbations of 27 km by 27 km by 1 km deep are used. The magnitude of the perturbations is either +1 or -1 g kg^{-1} (equivalent to about 1° C change of dewpoint). These perturbations are evenly spaced across the bations are evenly spaced across the horizontal domain, giving 45×45=2025 different perturbations needed to cover the entire domain in addition to one control run with no perturbation, for a total of 2026 different runs to make. This ensemble of 2026 members is run simultaneously on the Lemieux supercomputer at the Pittsburgh Supercomputer Center. This computer consists of over 3000 alpha processors. Our problem is highly efficient from a parallelization standpoint as each member of the ensemble is run on one CPU, and the entire ensemble executes in about 7 hours of wall-clock time, the same time as a single run of the model on one processor.

Two complete ensembles were run, one using perturbations of +1 g kg^{-1} and one using perturbations of -1 g kg^{-1}. One reason for doing this is to assess how linear the sensitivity response is. For a purely linear response, the sensitivity to a +1 g kg^{-1} perturbation would be the same as that to a -1 g kg^{-1} perturbation, though of opposite sign (the sign of the sensitivity does depend on how this field is defined; if it is defined as a derivative, then the sign is the same for positive or negative perturbations, though the physical effect of positive and negative perturbations are opposite).

3. RESULTS SHOWING LINEAR SENSITIVITY

Because the perturbations are small in both magnitude and area coverage, forecasts from each forecast of the ensemble is nearly identical; however, measurable differences do exist. A sensitivity field is obtained by taking the difference between some defined response function (many of which can be defined) of the unperturbed forecast and each member of the ensemble. The value of the sensitivity field at some location is then simply the difference between the response function of the control run and the run with the perturbation at that location.

Figure 6 shows the sensitivity field derived from a response function, *J*, defined as the area average surface water vapor:

$$J = \frac{\sum_i (q_{vi})\Delta x \Delta y}{\sum_i \Delta x \Delta y} \quad (1)$$

where the summation is taken over all the surface grid points shown in the box in south central Oklahoma shown in Fig. 6 (in this case, a 27 by 27 km box). The sensitivity field, $S(x,y)$, is defined here as the difference between *J* for the control run and *J* for each perturbed run:

$$S(x,y) = 1000 \bullet (J(x,y) - J_{control}) \quad (2)$$

The box indicated in Fig. 6 for the response function is an area which did not have any precipitation. Choosing such an area simplifies the interpretation of the water vapor sensitivity field.

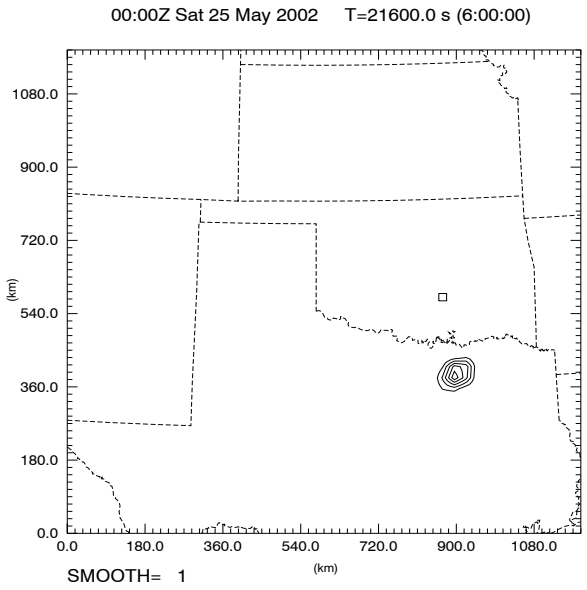

Fig. 6. Sensitivity field for the dependence on the area average surface water vapor inside the box indicated box to +1 g kg^{-1} perturbations in the initial condition. Units are .00002 g kg^{-1} per contour with a maximum of .00012 g kg^{-1}.

Figure 6 shows a well-defined, though modest, sensitivity of the water vapor forecast to perturbations in the water vapor field 6 hours earlier. The maximum sensitivity indicates that a 1 g kg^{-1} perturbation 200 km south of the area of interest (the box) led to an increase of .00012 g kg^{-1} in the area average surface water vapor in the box 6 hours later. The location and shape of the sensitivity contours indicate the combined effects of advection and diffusion in an expected manner. The region had southerly flow, so that the water vapor forecast depends on perturbations upstream. Also, diffusion, both numerical and physical, spreads the water vapor perturbation as might have been anticipated. The seemingly small sensitivity is due to the small initial q_v perturbations which are spread by diffusion over the 6 hours of model integration. Thus, the effect of any one initial perturbation on a small area in the forecast will be minimal. Complete ensembles were run using +1 g kg^{-1} and -1g kg^{-1} perturbations. The sensitivity field calculated from the -1 g kg^{-1} perturbation ensemble for the same response function as Fig. 6 is nearly identical to that obtained from the 1 g/kg perturbation ensemble. This implies a rather linear sensitivity for perturbations of this size in this region, a region which had no precipitation.

The calculation of the sensitivity field from (2) involves the subtraction of two numbers which are very close in magnitude. This necessarily leads to a loss of (for this case) 3 or 4 significant figures. Nonetheless, the well-defined sensitivity maximum in Fig. 6 shows that the technique is very sensitive, despite the loss of significant figures.

Figure 7 shows the sensitivity field for a different response function. In this case, *J* is defined as the area average of the total accumulated rainfall that fell in the box indicated throughout the 6 hours of integration. This box was selected to include the area of convection that initiated along the dryline. This shows that the convective rainfall near the area of initiation along the dryline depended on surface moisture to the southwest of the initiation location. It is interesting that the most sensitive area spans the initial dryline (see Figs.1 and 2), indicating that the low-level moisture on both side of the dryline at 18 UTC has similarly significant impact on precipitation in the box.

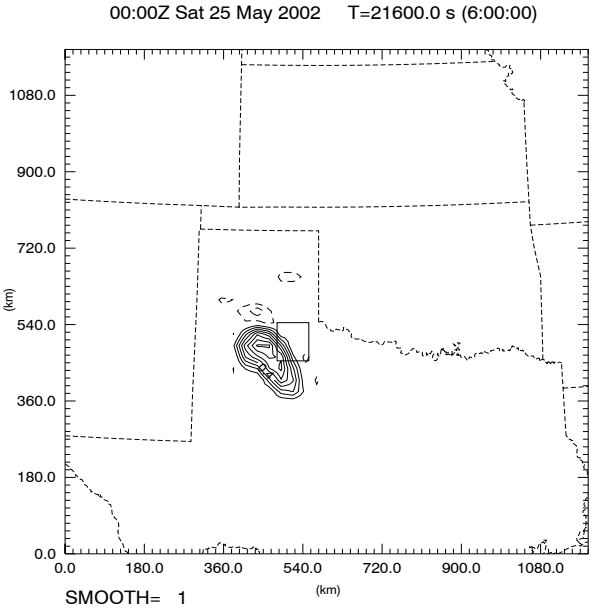

Fig. 7. Sensitivity field for the total area average accumulated precipitation in the indicate box to initial +1 g kg^{-1} water vapor perturbations. Contours are drawn every .1 mm, with a maximum of 0.8 mm.

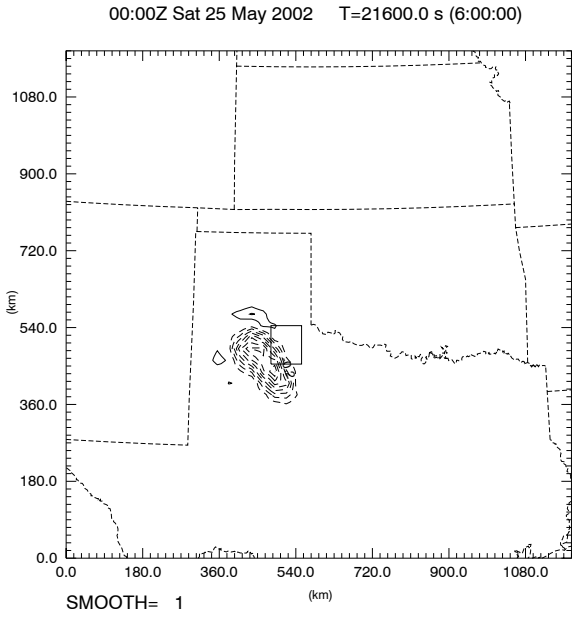

Fig. 8. As Fig. 7, but for -1 g kg^{-1} initial perturbations. Main local minimum is -0.9 mm.

Figure 8 shows the same sensitivity field as defined for Fig. 7, but calculated from the ensemble using -1 g kg^{-1} perturbations instead of +1 g kg^{-1}. The sensitivity pattern in Fig. 8 is very similar to that in Fig. 7, except for the sign difference. Figure 8 indicates precipitation reduction from the negative initial water vapor perturbations while in the previous case positive perturbations give rise to positive increase in precipitation. The very similar size and pattern of the sensitivity fields from these two cases indicate that the response of precipitation in the given box is very linear.

4. RESULTS SHOWING NONLINEAR SENSITIVITY

Figures 9 and 10 show the sensitivity fields for a response function defined as the area average accumulated precipitation that fell in the box shown in the figures. This box covers the area north and south of the cold front in Kansas and Oklahoma. For Figure 9, the ensemble using +1 g kg^{-1} perturbations was used, while for Figure 10, the -1 g kg^{-1} ensemble was used. Figure 9 shows two areas south of the initial front which have relatively strong impacts on the total precipitation, while Figure 10 is quite different showing much small areas of much reduced sensitivity. This implies a non-linear impact of perturbations initially south of the front.

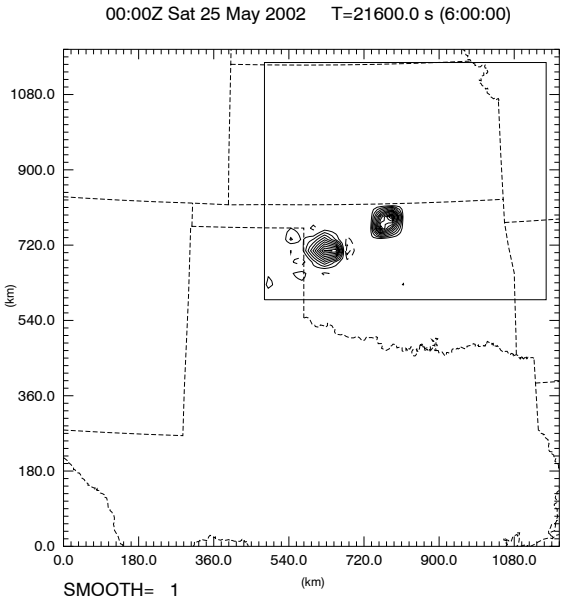

Figure 9. Sensitivity field derived from ensemble of 1 g/kg perturbations. Response function is total area average accumulated rainfall that fell in the box indicated. Contours are drawn every .02 mm. The maximum value of the two pronounced local maxima are about .25 mm.

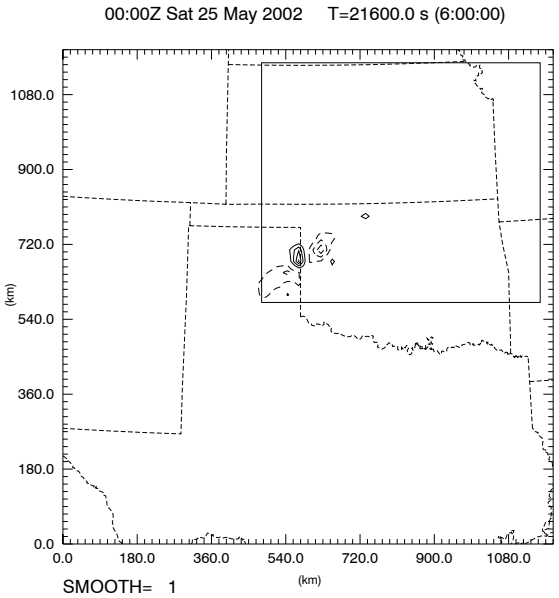

Figure 10. Same as Figure 9 but derived from the ensemble using -1 g/kg perturbations.

To more directly demonstrate this nonlinearity, two accumulated precipitation plots are made from individual members of the ensemble. Figure 11 shows the forecast accumulated precipitation from the ensemble member having its +1 g kg^{-1} moisture perturbation located at the local maximum in northwest Oklahoma in the sensitivity plot of Figure 9, and Figure 12 similarly shows the accumulated precipitation from the ensemble member located at the center of the local maximum seen in north-central Oklahoma in Figure 9. These two figures are to be compared with the unperturbed control run in Fig. 5. These two perturbed runs show a profound effect from the small initial perturbation. In Fig. 11, a precipitation maximum caused by a convective storm has appeared along the Kansas-Oklahoma border which did not exist in the control run, and in Fig. 12, another significant precipitation region has occurred, this time in southwest Kansas, which was not in the control either. These effects are highly nonlinear. The ensemble members using -1 g kg^{-1} moisture perturbations at the same locations as the 1 g kg^{-1} perturbations of Figs. 11 and 12 do not show any significant differences from the control run (Fig. 5).

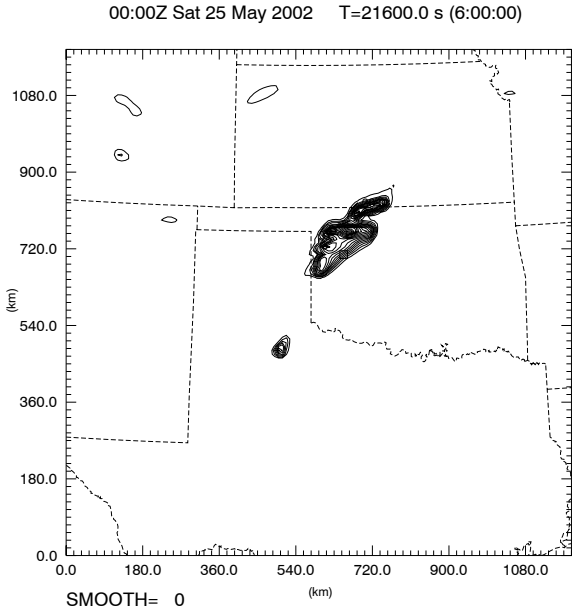

Figure 11. 6 hour forecast of accumulated precipitation from model run with an initial 1 g/kg surface moisture perturbation at the location indicated by a small box. Contour increments are 10 mm and the local maximum in the precipitation along the Kansas-Oklahoma border is 120 mm.

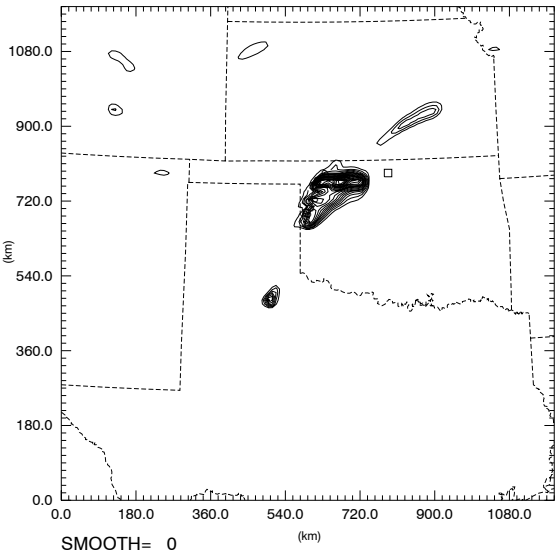

Figure 12. 6 hour forecast of accumulated precipitation from model run with an initial 1 g/kg surface moisture perturbation at the location indicated by a small box. Contour increments are 10 mm and the local maximum in the precipitation region in southeast Kansas is 30 mm.

Evidently, small positive perturbations at some locations can lead to entire storms which drop 10-100 mm of water, while negative perturbations at the same locations have no perceptible effect. This should be compared with the results of Crook (1996). Crook also found that perturbations of only 1 g kg^{-1} of moisture could make the difference between getting an intense storm and getting no storm at all. Crook, however, was perturbing a sounding which applied throughout the model domain. The results shown here indicate that small perturbations which are highly localized in space can have the same effect. The implications of this finding are that differences in the analysis of surface moisture that are within expected errors from such analyses, can make substantial differences in the forecast. Irrigation of a single farm could be enough to trigger a strong storm, and such variations are practically unmeasurable. This nonlinearity also implies that, at least for some cases, an adjoint analysis of sensitivity could be inaccurate and miss important sensitivities.

5. SUMMARY

This work has demonstrated the effectiveness of using a large ensemble to analyze forecast sensitivities to a two-dimensional initial field. Highly detailed sensitivity maps have been obtained which

show linear sensitivity responses of the advection and diffusion of water vapor in a southerly flow regime and of convection near the dryline, to low-level moisture perturbations 6 hours earlier. Some strong nonlinear sensitivities were found near the cold front.

The technique of using a large ensemble for sensitivity analysis has a number of advantages over using an adjoint:

1. Implementation is much easier.
2. No linearization assumption has to be made.
3. As no linearization approximation is made, a large ensemble can function as a validity test for adjoint-based sensitivity results.
4. Since no linearization is done, forecasts of any length can be considered.
5. The response function can be redefined after the calculations have been made, while in an adjoint-based sensitivity experiment the response function is fixed.

However, there are a number of disadvantages as well:

1. There is a need for a powerful parallel computer system in order to run the large number of forward model integrations in a reasonable amount of time.
2. To reduce the number of complete model runs needed, the number of degrees of freedom in the initial perturbations has to be reduced while an adjoint method can obtain complete sensitivity fields to all initial variables,
3. Storing results from a large number of 3D model runs poses a challenge, though this can be mitigated by only storing a small part of the output.

It is our plan to perform additional runs that examine sensitivities to initial perturbations in more variables and in other parts of the computational domain as well as to the boundary conditions. We also plan to conduct corresponding adjoint-based sensitivity experiments and compare the results from these two methods.

6. ACKNOWLEDGEMENTS

This research was supported by NSF grant ATM0129892. The second author was also supported by NSF grant ATM9909007 and a DOT-FAA grant. The computations were performed on the National Science Foundation Terascale Computing System at the Pittsburgh Supercomputing Center.

7. REFERENCES

Crook, N. Andrew, 1996: Sensitivity of moist convection forced by boundary layer process to low-level thermodynamic fields. *Mon. Wea. Rev., **124**, 1767-85.*

Errico, Ronald M., 1997: What is an adjoint model? *Bull. Amer. Meteor. Soc.,* **78**, 2577-91.

Errico, R. M., 2003: The workshop on applications of adjoint models in dynamic meteorology. *Bull. Amer. Meteor. Soc.*, **84**, 795-8.

Mullen, Steven L. and D. P. Baumhefner, 1994: Monte Carlo simulations of explosive cyclogenesis. *Mon. Wea. Rev.*, **122**, 1548-67.

Xue, M., K. K. Droegemeier, and V. Wong, 2000: The Advanced Regional Prediction System (ARPS) - A multiscale nonhydrostatic atmospheric simulation and prediction tool. Part I: Model dynamics and verification. *Meteor. Atmos. Physics*, **75,** 161-193.

Xue, M., K. Brewster, D. Weber, K. W. Thomas, F. Kong, and E. Kemp, 2002: Realtime storm-scale forecast support for IHOP 2002 at CAPS. *Preprint, 15th Conf. Num. Wea. Pred. and 19th Conf. Wea. Aanl. Forecasting*, San Antonio, TX, Amer. Meteor. Soc., 124-126.

Xue, M, D. Wang, J. Gao, K. Brewster and K. Droegemeir, 2003: The Advanced Regional Prediction System (ARPS), storm-scale numerical weather prediction and data assimilation. *Meteorol. Atmos. Phys.*, **82**: 139-170.